Article

Coordination Assembled Rings of Ferrocene-Bridged Trisporphyrin with Flexible Hinge-like Motion: Selective Dimer Ring Formation, Its Transformation to Larger Rings, and Vice Versa

Osami Shoji, Saori Okada, Akiharu Satake, and Yoshiaki Kobuke

J. Am. Chem. Soc., **2005**, 127 (7), 2201-2210• DOI: 10.1021/ja0445746 • Publication Date (Web): 01 February 2005

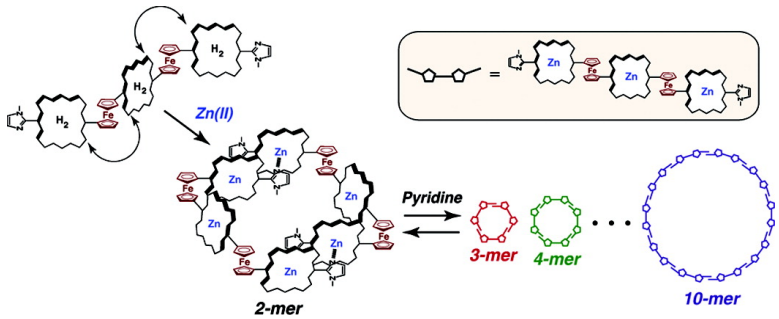

More About This Article

Additional resources and features associated with this article are available within the HTML version:

- Supporting Information
- Links to the 16 articles that cite this article, as of the time of this article download
- Access to high resolution figures
- Links to articles and content related to this article
- Copyright permission to reproduce figures and/or text from this article

View the Full Text HTML

J|A|C|S
ARTICLES
Published on Web 02/01/2005

Coordination Assembled Rings of Ferrocene-Bridged Trisporphyrin with Flexible Hinge-like Motion: Selective Dimer Ring Formation, Its Transformation to Larger Rings, and Vice Versa

Osami Shoji, Saori Okada, Akiharu Satake, and Yoshiaki Kobuke*

Contribution from the Graduate School of Materials Science, Nara Institute of Science and Technology, 8916-5 Takayama, Ikoma, Nara, 630-0101, Japan

Received September 8, 2004; E-mail: kobuke@ms.naist.jp

Abstract: Ferrocene-bridged trisporphyrin (**2**) was synthesized by two-steps condensation of corresponding aldehydes and dipyrromethanes, and its self-assembling behavior based on the complementary coordination motif of imidazolylporphyrinatozinc(II) was investigated in conjunction with hinge-like flexibility given by freely rotating cyclopentadienyl rings of ferrocene connector. Ferrocene-bridged trisporphyrin (**2**) spontaneously and exclusively generated the dimeric ring (**7**) upon simple zinc(II) insertion, indicating that the freely rotating hinge connector favored the smallest ring formation. Taking advantage of the unique hinge-like flexibility of ferrocene, we attempted to transform the dimer ring into a mixture of porphyrin macrocycles by reorganizing the structure cleaved once by pyridine. A series of porphyrin macrocycles from trimer to decamer can be separated into its components by preparative gel permeation chromatograms. Macrocycles obtained are kept stable in the absence of coordinating solvents. On the other hand, they were easily transformed to the dimer ring in the presence of coordinating solvents such as methanol, showing that the transformation is completely reversible and can be controlled by the choice of the solvent system. A series of porphyrin macrocycles was confirmed via covalent linking of each complementary coordination dimer pair by metathesis reaction in the presence of Grubbs's catalyst. The coordination behavior of the bidentate ligands with different spacer lengths toward the dimer ring revealed that only the bidentate ligand (**15**) with a spacer length that matched the facing central porphyrins was selectively accommodated inside the ring. Coordination assembled flexible rings with tunable cavities and multiple coordination sites will be used as versatile hosts for a wide variety of guest molecules.

Introduction

Supramolecular assembly promises to provide an easy approach for constructing even sophisticated molecular architectures from simple components and has been studied extensively for the last two dacades.[1] The supramolecular architectures with cyclic structure have attracted considerable attention due to their potential application in the areas of host−guest chemistry, molecular recognition, and catalysis.[2] Multi-porphyrin macrorings[3] have attracted enormous interest because porphyrins provide rigid frameworks with relatively easy synthetic approaches and a replaceable central metal ion to which one or two axial basic ligands can coordinate. Furthermore, their biological importance, as it was found that the antenna chlorophylls in photosynthetic bacteria are arranged into macrorings to absorb and transfer solar energy with great efficiency, makes them one of the attracting research targets.

Previously, we succeeded in constructing porphyrin macrorings composed of 10 and 12 porphyrins[4] by utilizing the complementary coordination motif of imidazolyl Zn(II)porphyrin.[5] The resultant rings mimic the structure of light-harvesting antenna complexes (B850 in LH2 and LH1).[6,7] In these porphyrin macrorings, two imidazolyl porphyrins were connected via *m*-phenylene groups so as to fix the dihedral angle

(1) (a) Lehn, J.-M. *Supramolecular Chemistry: Concept and Perspectives*; VCH: Weinheim, 1995. (b) Steed, J. W.; Atwood, J. L. *Supramolecular Chemistry*; John Wiley & Sons, Ltd.: Chichester, England, 2000.
(2) (a) Stang, P. J.; Olenyuk, B. *Acc. Chem. Res.* **1997**, *30*, 502−518. (b) Fujita, M. *Chem. Soc. Rev.* **1998**, *27*, 417−425. (c) Leininger, S.; Olenyuk, B.; Stang, P. J. *Chem. Rev.* **2000**, *100*, 853−908. (d) Holliday, B. J.; Mirkin, C. A. *Angew. Chem., Int. Ed.* **2001**, *40*, 2022−2043.
(3) (a) Anderson, S.; Anderson, H. L.; Bashall, A.; McPartlin, M.; Sanders, J. K. M. *Angew. Chem., Int. Ed. Engl.* **1995**, *34*, 1096−1099. (b) Peng, X.; Aratani, N.; Takagi, A.; Matsumoto, T.; Kawai, T.; Hwang, I-W.; Ahn, T. K.; Kim, D.; Osuka, A. *J. Am. Chem. Soc.* **2004**, *126*, 4468−4469. (c) Li, J.; Ambroise, A.; Yang, S. I.; Diers, J. R.; Seth, J.; Wack, C. R.; Bocian, D. F.; Holten, D.; Lindsey, J. S. *J. Am. Chem. Soc.* **1999**, *121*, 8927−8940. (d) Mongin, O.; Schuwey, A.; Vallot, M.-A.; Gossauer, A. *Tetrahedron Lett.* **1999**, *40*, 8347−8350. (e) Slone, R. V.; Hupp, J. T. *Inorg. Chem.* **1997**, *36*, 5422−5423. (f) Funatsu, K.; Imamura, T.; Ichimura, A.; Sasaki, Y. *Inorg. Chem.* **1998**, *37*, 1798−1804. (g) Knapp, S.; Vasudevan, J.; Emge, T. J.; Arison, B. H.; Potenza, J. A.; Schugar, H. J. *Angew. Chem., Int. Ed.* **1998**, *37*, 2368−2370. (h) Haycock, R. A.; Hunter, C. A.; James, D. A.; Michelsen, U.; Sutton, L. R. *Org. Lett.* **2000**, *2*, 2435−2438. (i) Fukushima, K.; Funatsu, K.; Ichimura, A.; Sasaki, Y.; Suzuki, M.; Fujihara, T.; Tsuge, K.; Imamura, T. *Inorg. Chem.* **2003**, *42*, 3187−3193.
(4) (a) Takahashi, R.; Kobuke, Y. *J. Am. Chem. Soc.* **2003**, *125*, 2372−2373. (b) Ikeda, C.; Satake, A.; Kobuke, Y. *Org. Lett.* **2003**, *5*, 4935−4938.
(5) Kobuke, Y.; Miyaji, H. *J. Am. Chem. Soc.* **1994**, *116*, 4111−4112.
(6) (a) McDermott, G.; Prince, S. M.; Freer, A. A.; Hawthornthwaite-Lawless, A. M.; Papiz, M. Z.; Cogdell, R. J.; Isaacs, N. W. *Nature* **1995**, *374*, 517−521. (b) Papiz, M. Z.; Prince, S. M.; Howard, T.; Cogdell, R. J.; Isaacs, N. W. *J. Mol. Biol.* **2003**, *326*, 1523−1538. (c) Koepke, J.; Hu, X.; Muenke, C.; Schulten, K.; Michel, H. *Structure* **1996**, *4*, 581−597.

between the two porphyrins at around 120°. The convergent reorganization procedure promoted the formation of hexameric and pentameric macrorings.[4] Concurrently, we have been investigating the construction of porphyrin rings of any size to be utilized as host molecules for a variety of sizes of guest molecules[8] so that they could be accommodated and activated by light irradiation.

For this purpose, we needed a special porphyrin connector, which could adjust freely the dihedral angle on demand. Ferrocene is a well-known compound, not only for its high redox activity but also its unique rotational motion. The two cyclopentadienyl rings of ferrocene have a low rotational energy barrier, allowing almost free rotation,[9] and have been utilized to construct several molecular devices of unique functions.[10] Freely rotating cyclopentadienyl rings may give a hinge-like flexibility to a ferrocene-bridged porphyrin, making ferrocene the best candidate for the aforementioned porphyrin connector.

In the present work, we prepared ferrocene-bridged trisporphyrin with imidazole groups at both ends of the terminal porphyrin and explored its self-assembling behavior in conjunction with the hinge-like flexibility of ferrocene. We are particularly interested in how the hinge-like flexibility of ferrocene connector part can control the self-assembling structures.

Results and Discussion

Synthesis of Ferrocene-Bridged Trisporphyrin and Selective Dimer Ring Formation Simply by Zinc(II) Insertion. Ferrocene-bridged free base trisporphyrin (**2**) was prepared by two-steps condensation (Scheme 1). The first condensation of 1-methyl-2-imidazolecarbaldehyde,[11] *meso*-(2-methoxycarbonylethyl)dipyrromethane,[12] and 1,1′-ferrocenedialdehyde[13] was performed in the presence of trifluoroacetic acid at room temperature. The oxidation with chloranil was performed after neutralization of the resulting acidic solution by triethylamine as ferrocene is easily oxidized under acidic conditions,[14] giving **1** in 5.1% yield. The second condensation of **1** and *meso*-(*n*-heptyl)dipyrromethane[15] gave **2** in 45% yield based on the amount of **1** used. Treatment of a chloroform solution of **2** (0.2 mM) with a methanol solution of zinc(II) acetate converted **2** to **2(Zn)**. Using ferrocenecarbaldehyde,[16] monomer porphyrins **5** and **5(Zn)** were also prepared.

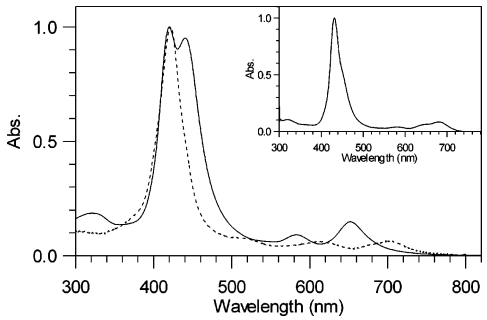

Figure 1. UV−vis spectra of **2** (broken line) and **2(Zn)** (solid line) in chloroform at room temperature. The inset shows the UV−vis spectrum of **2(Zn)** in pyridine. Cell length = 1 cm.

The UV−vis spectra of **2** and **2(Zn)** in chloroform are shown in Figure 1.[17] The UV−vis spectrum of **2(Zn)** showed splitting in the Soret band with peaks at 420.0 and 440.5 nm in accordance with the complementary dimer formation of imidazolyl porphyrin as reported previously.[5] In pyridine (inset of Figure 1), this splitting disappeared and the absorption spectrum similar to **2** was observed indicating that the complementary coordination was cleaved by pyridine coordination to result to a monomeric trisporphyrin. The GPC trace of **2(Zn)** showed a sharp single peak at 13.4 min that was clearly different from that of **2**, eluting at 13.9 min (Figure 2), showing the assembled structure of trisporphyrin. In addition, the sharp single peak was not accompanied by signals related to the polymeric porphyrin and formation of a single component is highly probable. This peak at 13.4 min was assigned to **7** (the dimer ring of **2(Zn)**) (Figure 4) as the ESI-TOF mass showed peaks at 1457.29 and 2186.50 corresponding to the trivalent and divalent cations, respectively (Figure 3). Because of the large association constant of complementary coordination (more than 10^{11} M^{-1}), two imidazolylporphyrinatozinc(II)'s at both ends of **2(Zn)** were brought into formation of the complementary dimer of ring structure.[18]

The ^{1}H NMR spectrum of **7** in tetrachloroethane-d_2 (Figure 5d) gave a complicated spectrum by the presence of several topological isomers with respect to ferrocene ("up" and "down") and the complementary coordination ("in−in" and "in−out") as shown in Scheme 2. As a result of a combination of two factors, the dimer ring possesses six possible topological isomers. Even so, based on HMQC and HH-COSY measurements (Figures S1 and S2 in the Supporting Information), β-pyrrole, ferrocene, and imidazole H_4 and H_5 protons could be assigned. Imidazole protons were observed at 2.82, 2.55, 1.42, and 0.90 ppm for H_4 and at 6.35 and 5.10 ppm for H_5, respectively. These peaks appeared obviously at higher fields in comparison to those of **2** observed at 7.72 and 7.45 ppm for H_4 and H_5, respectively (Figure 5c), clearly indicating the complementary dimer formation. In the case of complementary dimer of **5(Zn)**, imidazole protons appeared at 2.15 and 5.58 ppm for H_4 and H_5, respectively (Figure 5b).[19] Two kinds of

(7) (a) Walz, T.; Jamieson, S. J.; Bowers, C. M.; Bullough, P. A.; Hunter, C. N. *J. Mol. Biol.* **1998**, *282*, 833−845. (b) Jamieson, S. J.; Wang, P.; Qian, P.; Kirkland, J. Y.; Conroy, M. J.; Hunter, C. N.; Bullough, P. A. *EMBO J.* **2002**, *21*, 3927−3935. (c) Roszak, A. W.; Howard, T. D.; Southall, J.; Gardiner, A. T.; Law, C. J.; Isaacs, N. W.; Cogdell, R. J. *Science* **2003**, *302*, 1969−1972.
(8) For recent research on the self-assembled macrocycles with tunable cavity, see: (a) Jiang, H.; Lin, W. *J. Am. Chem. Soc.* **2003**, *125*, 8084−8085. (b) Jiang, H.; Lin, W. *J. Am. Chem. Soc.* **2004**, *126*, 7426−7427.
(9) Luke, W. D.; Streitwieser, A., Jr. *J. Am. Chem. Soc.* **1981**, *103*, 3241−3243 and references therein.
(10) (a) Inouye, M.; Hyodo, Y.; Nakazumi, H. *J. Org. Chem.* **1999**, *64*, 2704−2710. (b) Muraoka, T.; Kinbara, K.; Kobayashi, Y.; Aida, T. *J. Am. Chem. Soc.* **2003**, *125*, 5612−5613. (c) Li, C.; Medina, J. C.; Maguire, G. E. M.; Abel, E.; Atwood, J. L.; Gokel, G. W. *J. Am. Chem. Soc.* **1997**, *119*, 1609−1618. (d) Okamura, T.; Sakauye, K.; Ueyama, N.; Nakamura, A. *Inorg. Chem.* **1998**, *37*, 6731−6736.
(11) Milgrom, L. R.; Dempsey, P. J. F.; Yahioglu, G. *Tetrahedron* **1996**, *52*, 9877−9890.
(12) Ohashi, A.; Satake, A.; Kobuke, Y. *Bull. Chem. Soc. Jpn.* **2004**, *77*, 365−374.
(13) Balavoine, G. G. A.; Doisneau, G.; Fillebeen-Khan, T. *J. Organomet. Chem.* **1991**, *412*, 381−382.
(14) Gryko, D. T.; Zhao, F.; Yasseri, A. A.; Roth, K. M.; Bocian, D. F.; Kuhr, W. G.; Lindsey, J. S. *J. Org. Chem.* **2000**, *65*, 7356−7362.
(15) Tomohiro, Y.; Satake, A.; Kobuke, Y. *J. Org. Chem.* **2001**, *66*, 8442−8446.
(16) Mueller-Westerhoff, U. T.; Yang, Z.; Ingram, G. *J. Organomet. Chem.* **1993**, *463*, 163−167.
(17) The fluorescence of the porphyrin moieties in **2** and **5** is quenched to a large extent ($\Phi = 1.1 \times 10^{-3}$ and 0.3×10^{-3}, for **2** and **5**, respectively), and almost no fluorescence was observed after zinc(II) insertion, indicating efficient reductive quenching of adjacent ferrocene moiety.
(18) GPC measurement of **7** was carried out by changing the concentration in the range 0.1 mM to 3.1 μM ([**2(Zn)**]). No appreciable difference in the peak position and the shape was observed, indicating that the intermolecular interaction can be negligible in the concentration range examined.

Scheme 1. Synthetic Route to Ferrocene-Bridged Trisporphyrins and Molecular Structures of Monomer Porphyrins

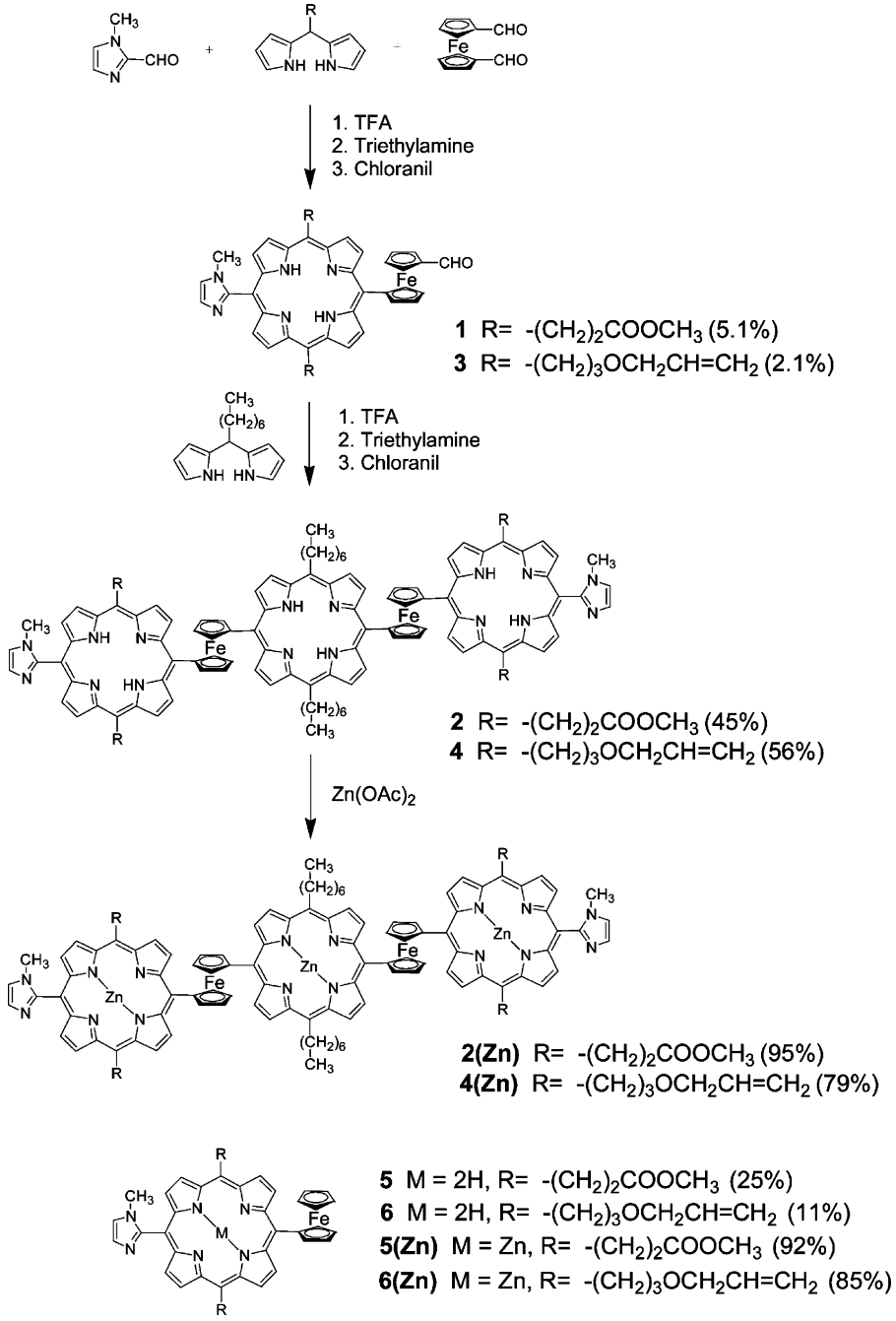

1 R= -$(CH_2)_2COOCH_3$ (5.1%)
3 R= -$(CH_2)_3OCH_2CH{=}CH_2$ (2.1%)

2 R= -$(CH_2)_2COOCH_3$ (45%)
4 R= -$(CH_2)_3OCH_2CH{=}CH_2$ (56%)

2(Zn) R= -$(CH_2)_2COOCH_3$ (95%)
4(Zn) R= -$(CH_2)_3OCH_2CH{=}CH_2$ (79%)

5 M = 2H, R= -$(CH_2)_2COOCH_3$ (25%)
6 M = 2H, R= -$(CH_2)_3OCH_2CH{=}CH_2$ (11%)
5(Zn) M = Zn, R= -$(CH_2)_2COOCH_3$ (92%)
6(Zn) M = Zn, R= -$(CH_2)_3OCH_2CH{=}CH_2$ (85%)

imidazole H_5 protons and two sets of imidazole H_4 protons at higher and lower fields may correspond to those ligating from inner and outer parts of the ring structure, respectively.

Because NMR measurements of **7** could not give clear information on the ring structure due to its complexity, we performed covalent linking of complementary coordination dimer using the ring-closing metathesis reaction to accumulate another evidence of the dimer ring structure. The ring-closing metathesis reaction using Grubbs's catalyst[20] has been widely used for the preparation of several polymers and ring structures and was also applied to connect supramolecules covalently.[21] We have already established a method linking covalently the complementary coordination dimer pair by using the ring-closing metathesis reaction, giving a conclusive proof of the dimer ring structure.[4b] To introduce olefinic groups at the *meso*-position, a conversion of methyl ester to allyl ester by transesterification using tin catalyst[22] was carried out first. However, we could not obtain the desired product. Instead, trisporphyrin with allyl ether substituents at *meso*-positions (**4**) was separately prepared in a manner similar to the synthesis of **2**. No difference in self-assembling behavior between trisporphyrin with 2-methoxy-

(19) The peaks of β-pyrrole (two of eight protons) and *N*-CH_3 protons of **5(Zn)** are also shifted to higher field caused by slipped cofacial dimer formation and appeared at 5.48 and 1.72 ppm, respectively (Figure 5b).

(20) (a) Schwab, P.; France, M. B.; Ziller, J. W.; Grubbs, R. H. *Angew. Chem., Int. Ed. Engl.* **1995**, *34*, 2039−2041. (b) Schwab, P.; Grubbs, R. H.; Ziller, J. W. *J. Am. Chem. Soc.* **1996**, *118*, 100−110.

(21) (a) Clark, T. D.; Ghadiri, M. R. T. *J. Am. Chem. Soc.* **1995**, *117*, 12364−12365. (b) Clark, T. D.; Kobayashi, K.; Ghadiri, M. R. T. *Chem.-Eur. J.* **1999**, *5*, 782−792. (c) Kim, Y.; Mayer, M. F.; Zimmerman, S. C. *Angew. Chem., Int. Ed.* **2003**, *42*, 1121−1126.

(22) Otera, J.; Danoh, N.; Nozaki, H. *J. Org. Chem.* **1991**, *56*, 5307−5311.

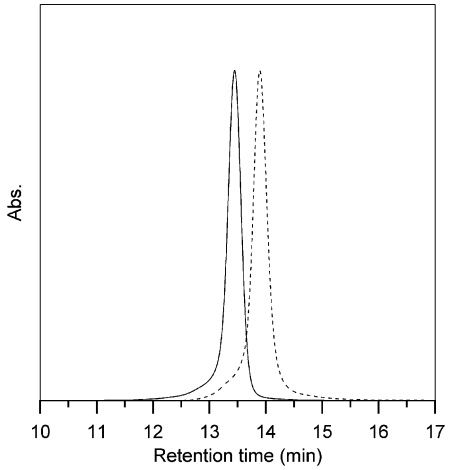

Figure 2. GPC traces of **2** (broken line) and **2(Zn)** just after zinc insertion (solid line).

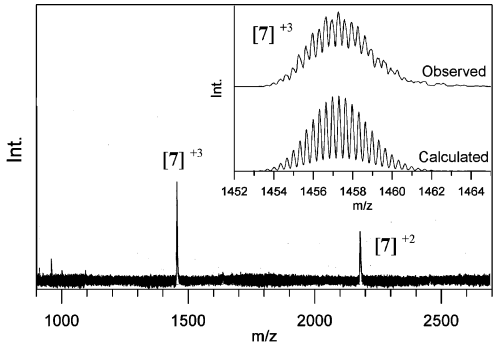

Figure 3. ESI-TOF mass spectrum of **7** (the dimer ring of **2(Zn)**).

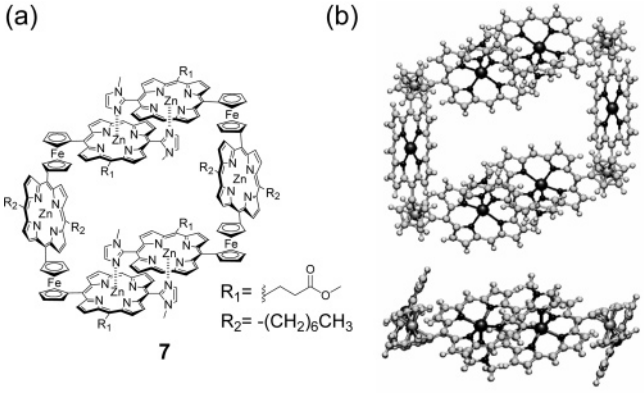

Figure 4. (a) The molecular structure of **7** (the dimer ring of **2(Zn)**) and (b) the molecular model of one of the topological isomers (*Sym 3* in Scheme 2) (top view (upper) and side view (lower)). The molecular model was obtained using the AM1 method in WinMOPAC Ver. 3.9 (Fujitsu Co. Ltd.). The substituents at the porphyrin *meso*-position were replaced by hydrogen atoms for simplicity.

carbonylethyl and 3-allyloxypropyl substituents was noted, and **4** afforded the complementary dimer of the ring structure (**8**) by simple zinc(II) insertion (GPC trace of **8** is shown in Figure S4 in the Supporting Information). The MALDI-TOF mass spectrum of **8** after the metathesis reaction showed a single peak at 4357.39 which was assigned to the dimer ring whose four reaction sites were fully reacted (**9**) (Scheme 3) (calcd molecular weight for $[M + H]^+$ 4357.38), in sharp contrast to that the MALDI-TOF mass gave only a monomeric peak at 2234.30 (peak maxima) before the metathesis reaction (Figure 6). The spectral shape agrees well with that of the calculated one,

Scheme 2. Schematic Representation of Six Possible Topological Isomers for **7**

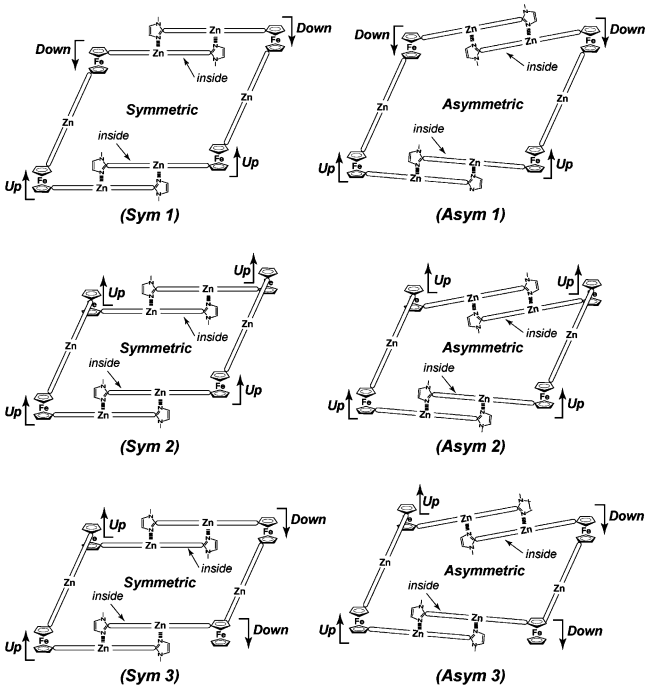

indicating that four ring-closing metathesis reactions completed in a pairwise linking between nearby *meso*-substituents. UV−vis spectra of **9** in chloroform and in pyridine were not much different, showing that the dimer ring structure was maintained even in coordinating solvent (Figure 7). Small differences in the spectral shape in pyridine arise from pyridine coordination to the central porphyrin of trisporphyrin as the covalently linked complementary coordination dimer alone gave virtually no spectral change.[12]

All of these findings are in a complete agreement with the proposed ring structure. A flexible hinge-like motion must have played a critical role in the selective dimer ring formation. When one complementary dimer is formed between two trisporphyrins, both ends of the resulting noncyclic dimer try to find their partner. With the flexible hinge-like motion of the ferrocene connection, it is much easier to find the opposite end[23] in the same molecule than the sites in other molecules because of its higher local concentration. The dimer ring formation without accompanying any polymeric components was a result of simple zinc insertion without use of any special techniques. The freely rotating hinge connector favored the formation of the smallest ring. In the case of trisporphyrin without the flexible hinge-like motion (*m*-phenylene-bridged trisporphyrin[24]), simple zinc insertion initially gave a polymeric mixture even under more dilute conditions (7.2 μM), clearly showing that the flexible ferrocene connector is essential to specific dimer formation.

Reorganization into Larger Rings. By utilizing the unique rotational behavior of ferrocene, we tried to reorganize the specific dimer into other forms. **7** was first dissolved in pyridine

(23) Kinetics of end-to-end collisions in a short peptide with a fluorophore and a quencher at each end has been examined by Nau et al. They observed significant intramolecular quenching in the case of flexible connector caused by frequent collision in comparison to that of ridged connector. See: Hudgins, R. R.; Huang, F.; Gramlich, G.; Nau, W. M. *J. Am. Chem. Soc.* **2002**, *124*, 556−564.

(24) Kuramochi, Y.; Satake, A.; Kobuke, Y. *J. Am. Chem. Soc.* **2004**, *126*, 8668−8669.

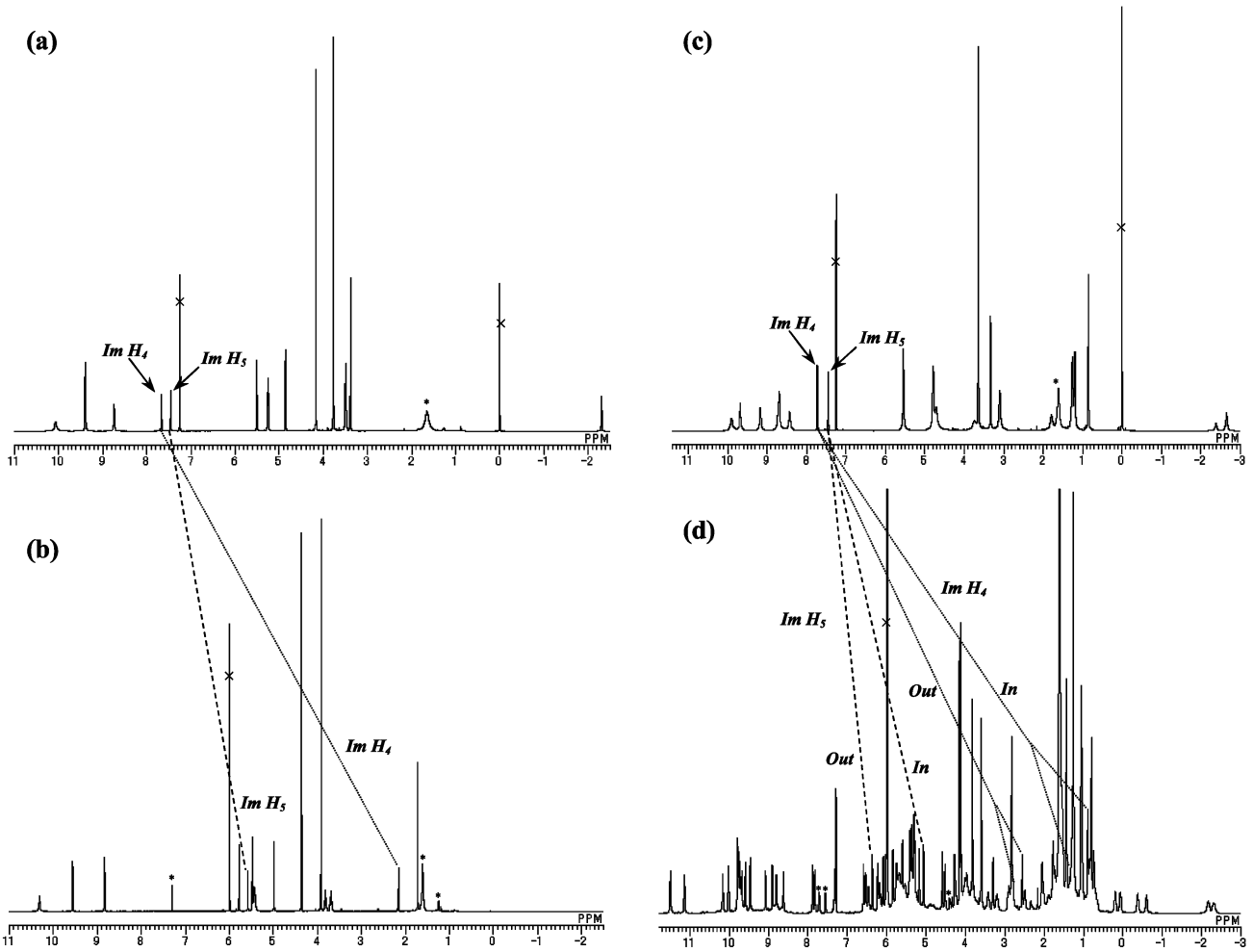

Figure 5. ^{1}H NMR spectra of **5** (a) and **2** (c) in $CDCl_3$ and **5(Zn)** (b) and **7** (d) in tetrachloroethane-d_2 at room temperature. "*" denotes impurity.

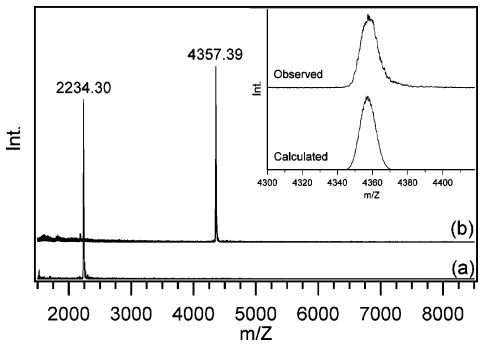

Figure 6. MALDI-TOF mass spectra of **8** (a) and that after metathesis reaction (b). The inset shows magnified spectra in comparison to that calculated for **9** (the covalently linked **8**, $C_{244}H_{233}Fe_4N_{32}O_8Zn_6$).

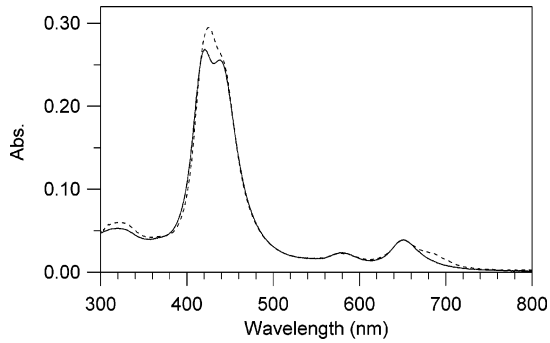

Figure 7. UV−vis spectra of **9** in chloroform (solid line) and in pyridine (broken line) at room temperature. Cell length = 1 cm.

to dissociate into pyridine-coordinated monomer **2(Zn)** (Scheme 4). Pyridine was then evaporated to dryness to leave the solid sample, whose chloroform solution, containing 0.5% ethanol as a stabilizer, showed a dramatic change of size distribution upon simply standing. A large peak was observed initially at the exclusion limit (ca. 8 min), with strong tailing, indicating that almost all of the dimer was transformed into a polymeric mixture of large molecular weights by this treatment (Figure 8, thick line). When this polymer was left standing in solution, the sharp peak at the exclusion limit disappeared rapidly (after 1 h) to give broad peaks at longer retention times corresponding to a polymer mixture of lower molecular weights. This broad peak shifted day by day to longer retention times and further to show the distribution of well-separated peaks of lower molecular weights after a week, leading the distribution finally to the predominant amount of **7** after 70 days. The rate process was accelerated by simply adding methanol (chloroform/methanol = 1/1), and all of the structures obtained after pyridine treatment could be transformed into **7** within 2 days.[25] Therefore, the transformation is completely reversible and can be controlled simply by the choice of the solvent system. We attempted to

(25) Methanol weakly competes with the imidazolyl group for the coordination to the zinc(II) and thus accelerates the exchanging of the partner in the complementary coordination.

Scheme 3. Covalent Linking of **8**

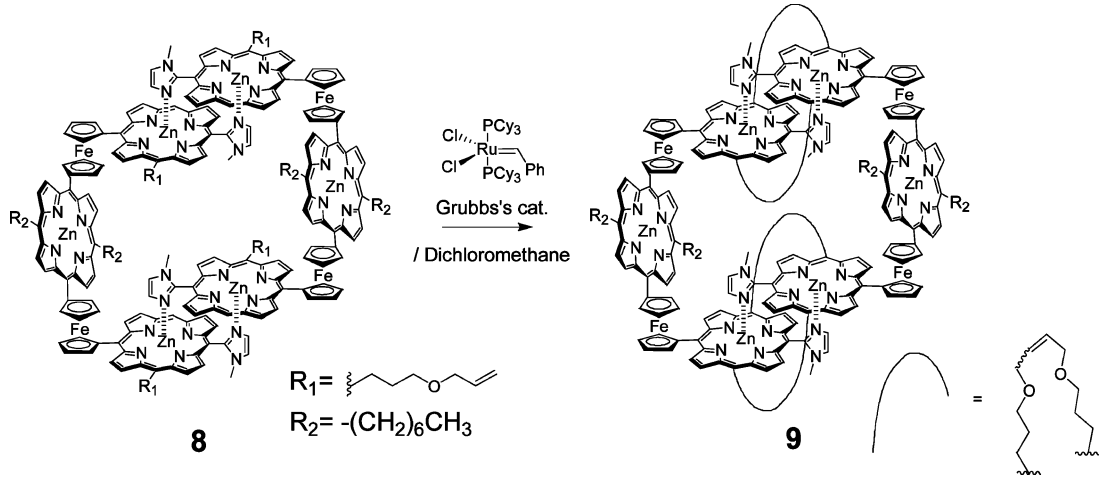

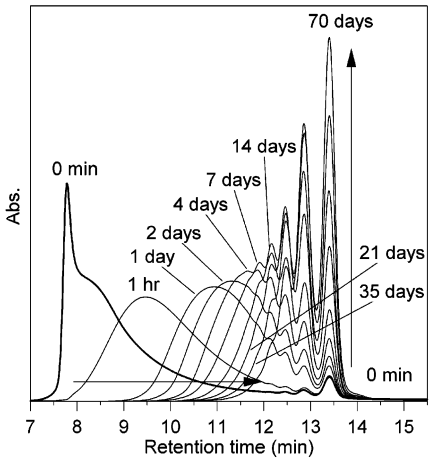

Figure 8. (a) Time-dependent change of GPC chromatograms in the reorganization process. The chloroform solution (including 0.5% of ethanol) of the sample after reorganization was left standing at room temperature in the dark. [**2(Zn)**] = 0.4 mM. Times are 0 min (thick line) (the sample immediately after the reorganization), 1 h, 1 day, 2 days, 4 days, 7 days, 14 days, 21 days, 35 days, and 70 days.

Scheme 4. Reorganization of **7**

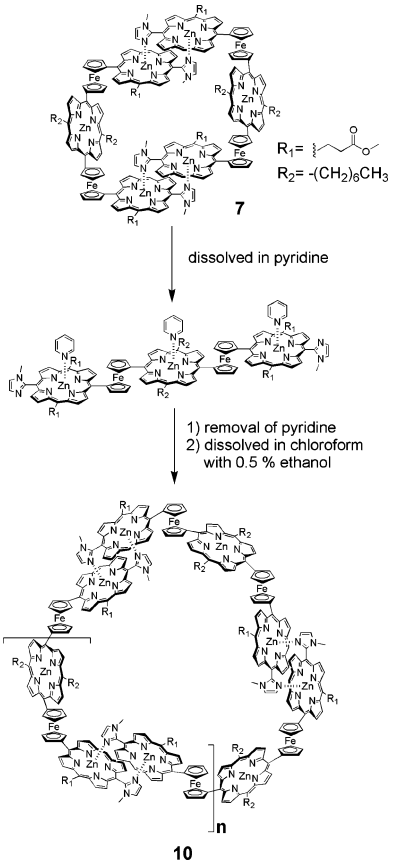

separate the components of the sample after it had been standing for 4 days by preparative GPC. Peaks eluting earlier than dimer were recycled twice, and eight peaks, tentatively assigned to 10-mer, 9-mer, 8-mer, 7-mer, 6-mer, 5-mer, 4-mer, and 3-mer, were fractionated (Figure 9a). The GPC traces of isolated components gave sharp peaks, allowing clear discrimination of all of the components (Figure 9b). In addition, a plot of the retention time of each peak maximum against the logarithm of the calculated molecular weight gave a straight line (Figure 9c), suggesting that a series of rings (**10**) up to a decamer was successfully isolated.[26] These peaks maintained sharp elution behavior with GPC when kept as solids or in dichloromethane solution, unless coordinating solvents were added. It is noteworthy that this series of rings are easily equilibrated in the presence of coordinating solvents and at the same time they are kept stable in their absence. The story of the reorganization is schematically shown in Scheme 5.

Unfortunately, neither ESI-TOF nor MALDI-TOF mass spectra of the isolated compounds gave any information about the number of trisporphyrin units. The former did not afford any peak, and the latter afforded only the peak of monomeric trisporphyrin. To overcome this situation, trisporphyrin **4(Zn)** with terminal olefins was similarly reorganized to determine the molecular weight and thus the number of trisporphyrin units of a series of reorganized samples by ring-closing metathesis reaction (Scheme 6). When the reorganized mixture (**11**) was stirred with Grubbs's catalyst, the MALDI-TOF mass spectrum

(26) The ^{1}H NMR spectrum of the mixture of larger rings (the region from $\mathbf{10}_{(3-\mathrm{mer})}$ to $\mathbf{10}_{(10-\mathrm{mer})}$ was collected by preparative GPC with two recycling processes) in tetrachloroethane-d_2 gave a relatively simple spectrum (Figure S5 in the Supporting Information). Although each peak was too broad to give clear signals in HMQC and HH-COSY spectra, we could assign the peaks at around 5.4 ppm to β-pyrrole protons that are shifted to higher field as a result of complementary coordination. The absence of N-CH_3 protons at 3.3 ppm and the presence of β-pyrrole protons at around 5.4 ppm strongly suggest that all of the imidazolylporphyrinatozinc(II) in trisporphyrin formed a complementary dimer and the absence of noncyclic structure in the mixture of larger rings.

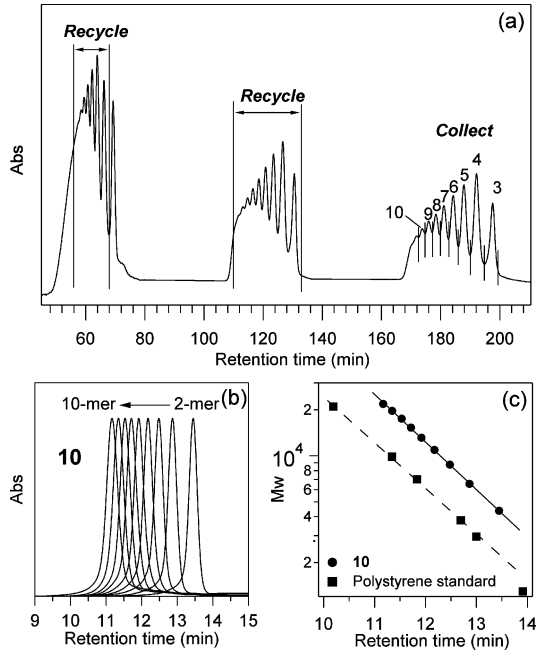

Figure 9. (a) Preparative GPC of the reorganized mixture with two recycling processes using chloroform as eluent. Numbers denote the number of **2(Zn)** units. (b) GPC analysis of **10** (a series of rings) obtained after isolation. Traces are normalized at peak maxima. (c) Plots of the logarithm of molecular weight of **10** (●) and polystyrene standard (■) against the retention time.

(Figure 10a) gave a series of peak maxima at 4357.29, 6535.84, 8713.38, 10 892.19, 13 070.07, 15 248.59, 17 426.49, 19 603.26, and 21 783.72 (*m*/*z*), which agreed well with the calculated molecular weights for covalently linked macrocycles (**12**) ([M + H]$^+$ calcd molecular weight for **12**$_{(3-mer)}$, 6535.58; **12**$_{(4-mer)}$, 8713.77; **12**$_{(5-mer)}$, 10 891.97; **12**$_{(6-mer)}$, 13 070.16; **12**$_{(7-mer)}$, 15 248.35; **12**$_{(8-mer)}$, 17 426.54; **12**$_{(9-mer)}$, 19 604.73; **12**$_{(10-mer)}$, 21 782.92). The series of compounds are thus assigned to macroring structures.

To accumulate further proof of the ring structure for these series, noncyclic compounds were prepared by mixing **4(Zn)** with monomer porphyrin **6(Zn)** in a 1:2 molar ratio and applying the reorganization procedure using pyridine to generate **13** (a series of oligomers terminated at either end by **6(Zn)**) (Scheme 6). When this mixture was subjected to the ring-closing metathesis reaction, the MALDI-TOF mass spectrum (Figure 10b) gave peaks at 1613.21, 3791.19, 5969.09, 8147.47, and 10 325.21 (*m*/*z*), matching the covalently linked noncyclic structures (**14**) ([M + H]$^+$ calcd molecular weights for **14**$_{(n=0)}$ (the covalently linked dimer of **6(Zn)**), 1613.13; **14**$_{(n=1)}$, 3791.33; **14**$_{(n=2)}$, 5969.52; **14**$_{(n=3)}$, 8147.71; **14**$_{(n=4)}$, 10 325.90). It is noteworthy that noncyclic structures are not accompanied by any appreciable peaks of ring components. Similarly to the case of **10**, we separated a series of covalently linked rings (**12**) as well as noncyclic structures (**14**) into their components by preparative GPC. The analytical GPC traces of each isolated component gave a sharp single peak (Figure 11), and their MALDI-TOF mass spectra gave the peaks corresponding to the single components up to **12**$_{(8-mer)}$ for the ring structure and up to **14**$_{(n=4)}$ for the noncyclic structure. Reflecting the structural difference, the plot of the retention time against the logarithm of molecular weight gave two different straight lines with an identical slope, that is, the line of noncyclic structure located below that of the rings. The shorter retention times observed for noncyclic species as compared to the rings are fully consistent with the general tendency that the former occupies larger exclusion volumes than the latter. The noncyclic compounds prepared similarly by reorganization of **2(Zn)** in the presence of **5(Zn)** also show GPC behavior similar to that of **13** (Figure S7 in the Supporting Information).

All of these results gave the conclusive evidence that ferrocene-bridged trisporphyrin can be reorganized into a series of porphyrin macrocycles by simple treatment with pyridine.[27] Long polymers observed initially were transformed immediately into a mixture of macrocycles on being dissolved in chloroform. Both ends of the initial linear polymer are terminated by pyridine coordination and substituted by complementary coordination on finding the counterpart at the other terminal or in the middle of the polymer. The flexible motion required for finding the counterpart is endowed by the freely rotating ferrocene hinge. The resulting larger ring can still find the counterpart in the middle of its own to reduce the ring size, but the reverse enlargement process must be unfavorable because of the intermolecular nature. Therefore, the transformation is vectorial from larger rings to smaller ones. Certainly, the transformation is assisted by weak ligation of ethanol to zinc(II). Without ethanol, rings are stable for many days. In the whole process, flexible hinge-like motion of ferrocene connector contributes greatly to the formation of porphyrin macrocycles, their unique transformation, and their stability.

Selective Binding of the Guest Molecule. Even after organization by complementary coordination, **7** still possesses two additional coordination sites available at the central Zn(II)porphyrin in the trisporphyrin. The coordination behavior of the bidentate ligands with different spacer length was investigated by UV−vis titration. Because **7** may possess several topological isomers as we described earlier, bidentate ligands with moderate flexibility (**15** and **16**, Scheme 7) were prepared so as to be accommodated cooperatively irrespective of small differences in distance and angle between two facing porphyrins among topological isomers. In Figure 12 are shown UV−vis spectral changes upon addition of bidentate ligands **15** and **16** as well as *N*-methylimidazole. The bidentate ligand **15** induced a clear spectral change with an isosbestic point at 660 nm (Figure 12a), showing that all topological isomers behaved similarly. Job's plot (Figure S11d) shows that **15** was bound into **7** with 1 to 1 stoichiometry. The binding constant of **15** was estimated to be 3.6×10^4 M^{-1}.[28] The bidentate ligand **16** behaved similarly in the spectral change during titration to *N*-methylimidazole ($K = 2.4 \times 10^3$ M^{-1}). Therefore, the binding constant was evaluated similarly as 1.8×10^3 M^{-1}. The larger binding constant observed for **15** is a positive sign for cooperative binding inside the ring, because selectivity on spacer length was observed. The relatively weak cooperativity comes partly from sterically crowded interior of **7** as suggested by the semiempirical MO calculation (Figure 4b). Another factor is

(27) Atomic force microscope (AFM) measurements of **10**$_{(10-mer)}$ casted onto mica substrate gave mostly circular images with relatively uniform diameters, along with larger ones arising presumably from the aggregated form (Figure S8). An averaged diameter and height for 32 isolated spots are 33.7 ± 2.6 and 0.83 ± 0.13 nm, respectively. Taking the curvature of the AFM probe (ca. 10 nm) in radius into consideration, the net diameter corrected is comparable to the calculated size of the ring (ca. 11 nm). As **10**$_{(10-mer)}$ may take many conformations, we estimated the size of the perfectly regular and circular ring structure of **10**$_{(10-mer)}$ instead of the average size of rings by using the molecular model (Figure S9).

(28) Connors, K. A. *Binding Constants: The Measurement of Molecular Complex Stability*; John Wiley & Sons: New York, 1987.

Scheme 5. Schematic Representation of the Reorganization Behavior of Ferrocene-Bridged Trisporphyrin[a]

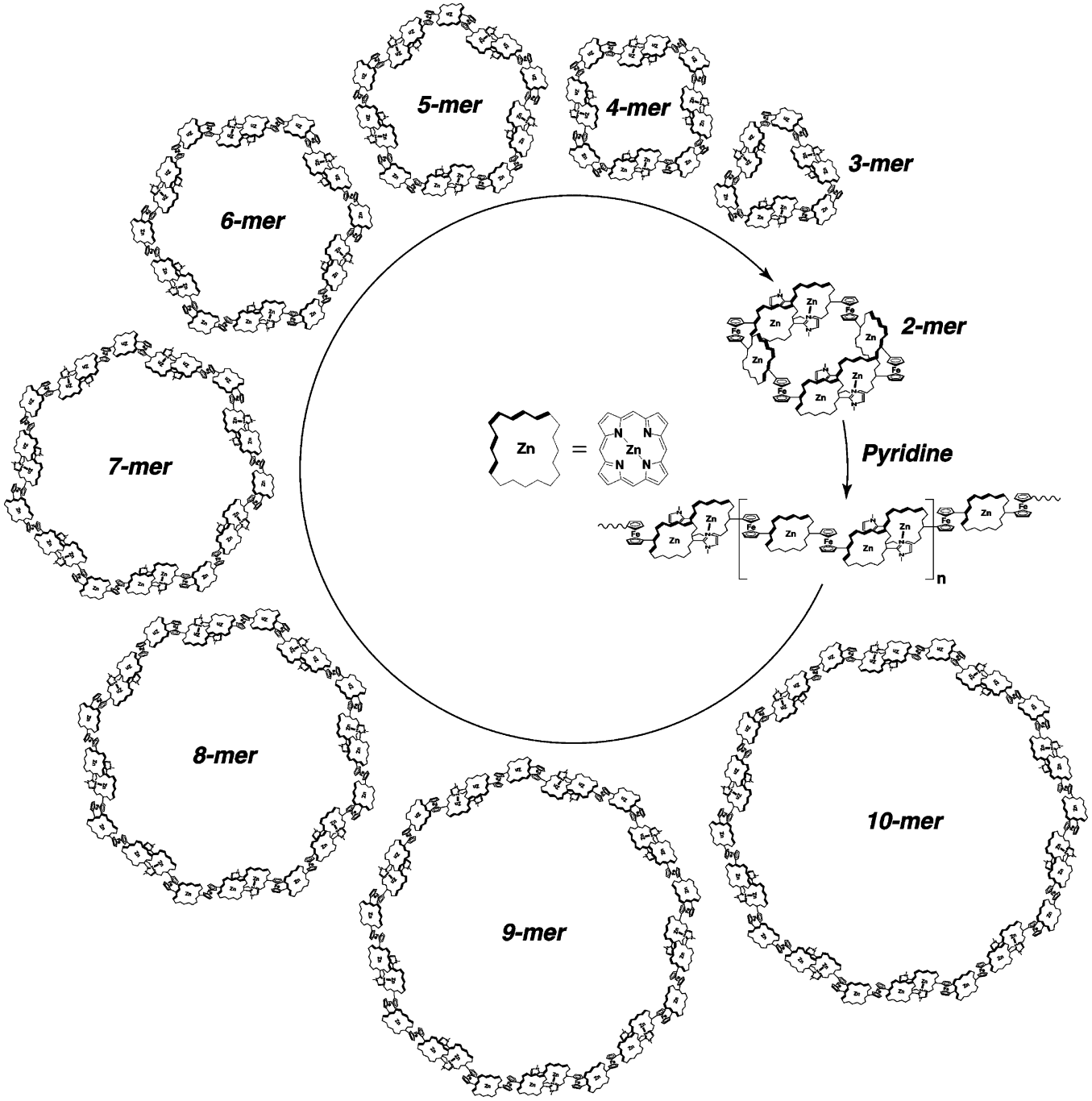

[a] All of the rings expressed in perfect ring structures do not necessarily express the real conformational structure.

the use of flexible ligand **15** for the reason described above. However, strong cooperative binding is expected to **10**$_{(3-\mathrm{mer})}$ and/or larger rings having enough space to accommodate the guest molecule without steric repulsion, similar to our porphyrin macrocycle reported recently.[24]

Conclusion

In this study, we have observed specific formation of a cyclic dimer by complementary coordination of imidazolylporphyrinatozinc(II) in ferrocene-bridged trisporphyrin and its conversion to a series of macrocycles, from trimer to decamer, through polymeric porphyrins. We have succeeded in confirming a series of macroring structures by covalent linking of neighboring *meso*-olefinic substituents in the complementary coordination pair using ring-closing metathesis reaction. The behavior of the covalently linked macrocycles on GPC differs obviously from that of noncyclic structures. The decamer cycle contains 30 porphyrin and 20 ferrocene units and provides multiple coordination sites. We believe that the hinge-like flexibility of ferrocene plays the most critical role in constructing these unique self-assembled structures and in conferring a unique dynamic behavior to the molecule in addition to unique coordination characteristics, allowing high stability and dynamic nature at the same time. Tunable, flexible, and large molecular cavities with multiple coordination sites make these macrocycles

Scheme 6. A Series of Rings with Allyl Ether Substituents at *meso*-Positions (**11**) Prepared from **8** Similarly to That of **10** and a Series of Corresponding Noncyclic Structures (**13**) Prepared by Treating a Mixture of **4(Zn)** and **6(Zn)** in a 1:2 Molar Ratio with Pyridine[a]

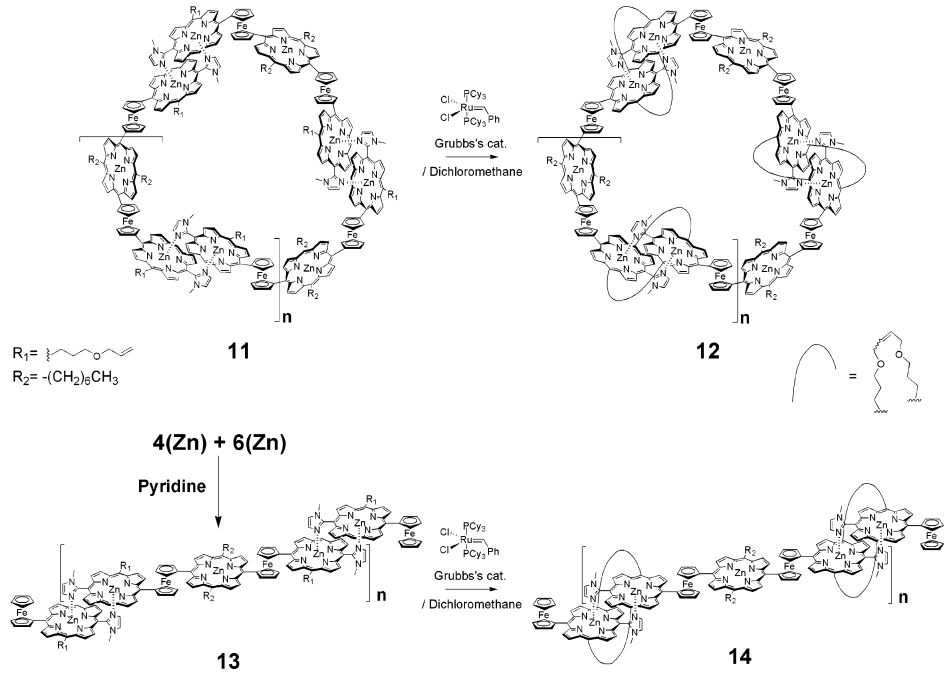

[a] The ring-closing metathesis reaction was carried out in the same manner as that for **8** (see the Supporting Information).

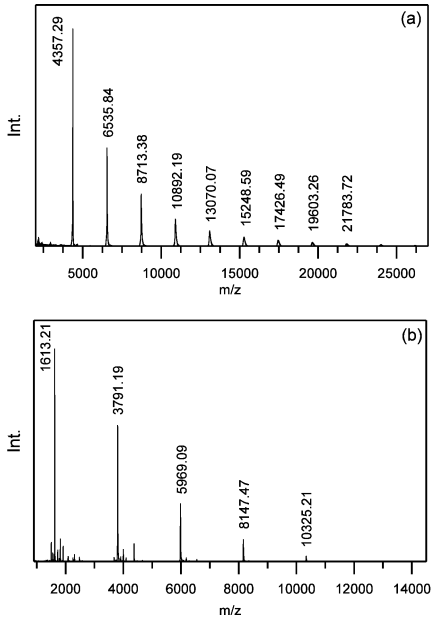

Figure 10. MALDI-TOF mass spectra of (a) a series of covalently linked rings (**12**) and (b) a series of covalently linked noncyclic structures (**14**).

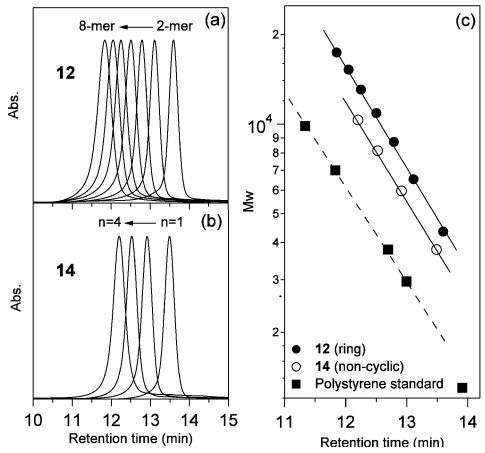

Figure 11. GPC analysis of (a) a series of covalently linked rings (**12**) and (b) a series of covalently linked noncyclic structures (**14**) obtained after isolation. Traces are normalized at peak maxima. (c) Plots of the logarithm of molecular weight of **12** (●), **14** (○), and polystyrene standard (■) against the retention time.

versatile hosts for a wide variety of guest molecules. Their potential use for elucidating the molecular recognition mechanism with cooperative and/or induced-fit binding also makes the series of assemblies attractive. Of course, porphyrin and ferrocene should play central roles due to their photo- and electrocatalytic functions.

Experimental Section

Measurements. ^{1}H and ^{13}C NMR spectra were recorded on a JEOL ECP-600 (600 MHz) spectrometer. The chemical shifts are reported in parts per million (ppm) using tetramethylsilane (TMS) or the residual protium in the NMR solvent as an internal reference. Assignments have been performed on the basis of COSY, HMQC, and DEPT measurements. The peaks overlapping with the residual water signal were assigned by using DANTE pulse sequence. UV−vis and steady-state fluorescence spectra were recorded on a Shimadzu UV-3100PC spectrophotometer and on a HITACHI F-4500 fluorescence spectrophotometer, respectively. Fluorescence quantum yields were estimated by comparison of integrated emission spectra with tetraphenylporphyrin in benzene ($\Phi_f = 0.11$) as a standard.[29] MALDI-TOF mass spectra were measured on a Perspective Biosystems Voyager DE-STR or KRATOS AXIMA with dithranol (Aldrich) as a matrix. ESI-TOF mass spectra were measured on JEOL AKI TOF. Analytical gel permeation chromatograms were obtained on a Hewlett-Packard HP1100 series equipped with an analytical JAIGEL 3HA column (Japan Analytical Industry Co. Ltd., 8 mm × 500 mm, exclusion limit: 70 000 Da). The atomic force microscope image was obtained on a Nanoscope IIIa

(29) Seybold, P. G.; Gouterman, M. *J. Mol. Spectrosc.* **1969**, *31*, 1−13.

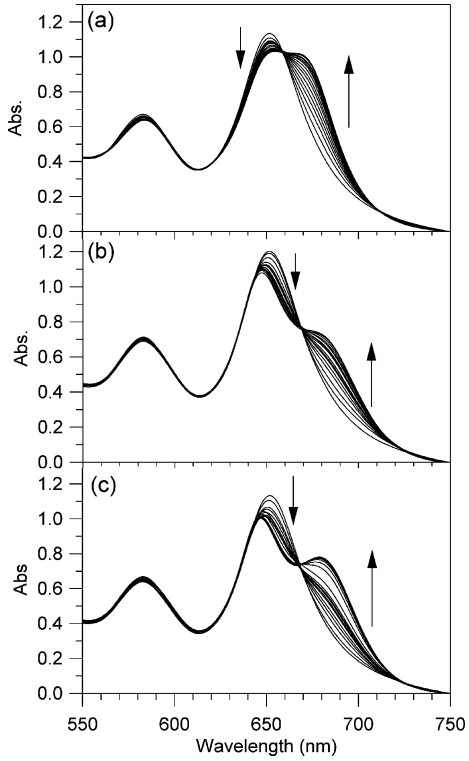

Figure 12. UV−vis spectral change in **7** in chloroform induced by addition of **15** (a), **16** (b), and *N*-methylimidazole (c) at room temperature. [**7**] = 5.6×10^{-5} M (**15**), 6.4×10^{-5} M (**16**), and 5.8×10^{-5} M (*N*-methylimidazole**)**. [**15**]/[**7**] = 0, 0.2, 0.4, 0.6, 0.8, 1.0, 1.2, 1.4, 1.6, 1.8, 2.0, 2.2, 2.4, 2.6, 2.8, 3.0. [**16**]/[**7**] = 0, 1, 2, 3, 4, 5, 6, 7, 8, 9, 10, 12, 14, 16, 18, 20. [**NMeIm**]/[**7**] = 0, 1, 2, 3, 4, 5, 6, 7, 8, 9, 10, 20, 30, 40, 50, 60, 70, 80. Cell length = 2 mm.

Scheme 7. Molecular Structures of Guest Molecules

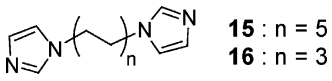

15 : n = 5
16 : n = 3

(Digital Instruments Co.) according to a tapping mode with a Si cantilever (a spring constant of 40 N m^{-1}, tip curvature radius of 10 nm).

General Methods. Column chromatography was performed using silica gel (silica gel 60N (spherical, neutral) 63-210 mm, KANTO chemical Co., Inc.) and aluminum oxide (aluminum oxide 90 active basic (0.063−0.200 mm), Merck Ltd.). Preparative gel permeation chromatograms were carried out on a recycling GPC-HPLC system with JAIGEL 3H columns (Japan Analytical Industry Co. Ltd., 20 mm × 600 mm, exclusion limit: 70 000 Da).

Molecular Modeling. The molecular models were obtained using the semiempirical MO calculation with geometry optimization (AM1[30] method in WinMOPAC Ver. 3.9 (Fujitsu Co. Ltd.)[31]). The calculations were carried out as follows. First, the geometries of 5,15-bis(ferrocenyl)-porphyrinatozinc(II), 1,1′-bis(porphyrinatozinc(II)-5-yl)ferrocene, and the complementary dimer of 5-ferrocenyl-15-(1-methylimidazol-2-yl)-porphyrinatozinc(II) were optimized using the AM1 method. Next, based on the geometries obtained above, the initial structures of **7** were created using Cerius[2] ver. 4.6 MatSci and optimized using the AM1 method, where the substituents at the porphyrin *meso*-position were replaced by hydrogen atoms for simplicity.

UV−Vis Titration and Job's Plot of 7. To a solution of **7** in chloroform was added a solution of the guest molecules in chloroform, and UV−vis spectra were recorded at 25 °C. All spectra were corrected with a dilution factor, and Δ*Abs* was plotted against [**15**]/[**7**], ([**16**] × 2)/[**2(Zn)**], and [*N*-methylimidazole]/[**2(Zn)**], respectively. The binding constant of **15** was estimated by curve fitting, assuming 1:1 complexation of **7**/**15** according to the literature.[28] As the two coordination sites in **7** seemed to behave independently against **16** and *N*-methylimidazole, the binding constant of **16** was estimated assuming 1:1 complexation of **2(Zn)**/(*N*-methylimidazolyl group) where **16** was regarded as two equimolar amounts of imidazolyl groups. The binding constant of *N*-methylimidazole was estimated similarly assuming 1:1 complexation of **2(Zn)**/(*N*-methylimidazole). Job's plot for the **7**/**15** complex was obtained from the UV−vis spectral change at 667 nm in chloroform.

Acknowledgment. This work was supported by CREST (Core Research for Evolutional Science and Technology) of the Japan Science and Technology Agency, Japan, and Grant-in-aid for Scientific Research 15205020.

Supporting Information Available: Experimental details for synthesis, NMR data (HMQC and HH-COSY of **7**, HMQC of **5(Zn)**, and ^{1}H NMR spectra of the mixture of larger rings, **10**$_{(3-mer)}$, **10**$_{(4-mer)}$, **10**$_{(5-mer)}$, **10**$_{(7-mer)}$, and **10**$_{(10-mer)}$), GPC analysis (**8** just after zinc insertion, the mixture of noncyclic structure prepared from **2(Zn)** and **5(Zn)**, and **11**−**14**), UV−vis spectra of **10**, AFM image and the molecular model of **10**$_{(10-mer)}$, curve-fitting analysis of **7** with **15**, **16**, and *N*-methylimidazole, and Job's plot for the **7**/**15** complex. This material is available free of charge via the Internet at http://pubs.acs.org.

JA0445746

(30) Dewar, M. J. S.; Zoebisch, E. G.; Healy, E. F.; Stewart, J. J. P. *J. Am. Chem. Soc.* **1985**, *107*, 3902−3909.
(31) Stewart, J. J. P. *MOPAC 2002*; Fujitsu Ltd.: Tokyo, Japan, 2001.